New $T=1$ effective interactions for the $f_{5/2}\,p_{3/2}\,p_{1/2}\,g_{9/2}$ model space: Implications for valence-mirror symmetry and seniority isomers

A. F. Lisetskiy,[1] B. A. Brown,[1] M. Horoi,[2] and H. Grawe[3]
[1]*National Superconducting Cyclotron Laboratory, Michigan State University, East Lansing, Michigan 48824-1321, USA*
[2]*Physics Department, Central Michigan University, Mount Pleasant, Michigan 48859, USA*
[3]*Gesellschaft für Schwerionenforschung mbH, D-64291 Darmstadt, Germany*
(Received 24 February 2004; published 25 October 2004)

New shell model Hamiltonians are derived for the $T=1$ part of the residual interaction in the $f_{5/2}\,p_{3/2}\,p_{1/2}\,g_{9/2}$ model space based on the analysis and fit of the available experimental data for $^{57}_{28}\mathrm{Ni}_{29}-^{78}_{28}\mathrm{Ni}_{50}$ isotopes and $^{77}_{29}\mathrm{Cu}_{50}-^{100}_{50}\mathrm{Sn}_{50}$ isotones. The fit procedure, properties of the determined effective interaction as well as new results for valence-mirror symmetry and seniority isomers for nuclei near ^{78}Ni and ^{100}Sn are discussed.

DOI: 10.1103/PhysRevC.70.044314 PACS number(s): 21.30.Fe, 21.10.Hw, 21.60.Cs, 27.40.+z

I. INTRODUCTION

Neutron-rich nickel isotopes in the vicinity of $^{78}_{28}\mathrm{Ni}_{50}$ are currently in the focus of modern nuclear physics and astrophysics studies [1–7]. The enormous interest in this region is motivated by several factors. The primary issue concerns the doubly magic nature of $^{78}_{28}$Ni and understanding the way in which the neutron excess will affect the properties of nearby nuclei and the ^{78}Ni core itself. The shell-model orbitals for neutrons in nuclei with $Z=28$ and $N=28-50$ (^{56}Ni-^{78}Ni) are the same as those for protons in nuclei with $N=50$ and $Z=28-50$ (^{78}Ni-^{100}Sn). Thus it is of interest to understand the similarities and differences in the properties of these nuclei with valence-mirror symmetry (VMS) [8]. The astrophysical importance is related to the understanding of the nuclear mechanism of the rapid capture of neutrons by seed nuclei through the r-process. The path of this reaction network is expected in neutron-rich nuclei for which there is little experimental data, and the precise trajectory is dictated by the details of the shell structure far from stability.

Experimental investigations of neutron-rich nuclei have greatly advanced the last decade providing access to many new regions of the nuclear chart. Nuclear structure theory in the framework of shell-model configuration mixing has also advanced from, for example, the elucidation of the properties of the *sd*-shell nuclei ($A=16-40$) in the 1980's [9] to those of the *pf*-shell ($A=40-60$) in current investigations [10–12]. Full configuration mixing in the next oscillator shell (sdg) is presently at the edge of computational feasibility. For heavy nuclei the spin-orbit interaction pushes the $g_{9/2}$ and $f_{7/2}$ orbits down relative to the lower-l orbits. Thus the most important orbitals for neutrons in the region of ^{68}Ni to ^{78}Ni are $p_{3/2}$, $f_{5/2}$, $p_{1/2}$, and $g_{9/2}$ (referred to from now on as the $pf_{5/2}g_{9/2}$ model space). It is noteworthy that this model space is not affected by center-of-mass spurious components. Full configuration mixing calculations for neutrons or protons in this model space are relatively easy. The work we describe here on the $T=1$ effective interactions will provide a part of the input for the larger model space of both protons and neutrons in these orbits where the maximum m-scheme dimension is 13,143,642,988. This proton-neutron model space is computationally feasible with conventional matrix-diagonalization techniques for many nuclei in the mass region $A=56-100$, and Quantum Monte Carlo Diagonalization techniques [13] or Exponential Convergence Methods [14] can be used for all nuclei.

The present paper reports on new effective interactions for the $pf_{5/2}g_{9/2}$ model space derived from a fit to experimental data for Ni isotopes from $A=57$ to $A=78$ and $N=50$ isotones from ^{79}Cu to ^{100}Sn for neutrons and protons, respectively. Predictions for the $^{72-76}$Ni isotopes are made using the new effective interaction. For the first time the calculated structures of the ^{68,70,72,74,76}Ni isotopes and the ^{90}Zr, ^{92}Mo, ^{94}Ru, ^{96}Pd, ^{98}Cd are compared and analyzed with respect to the VMS concept [8]. Our work provides a much improved Hamiltonian for $Z=28$ over those considered in smaller model spaces [1–3,15], and also provides a new Hamiltonian for $N=50$ that is similar to those obtained previously [16,17].

II. DERIVATION OF THE EFFECTIVE INTERACTION

The effective interaction is specified uniquely in terms of interaction parameters consisting of four single-particle energies and 65 $T=1$ two-body matrix elements (TBME). The starting point for the fitting procedure was a realistic *G*-matrix interaction based on the Bonn-C *N N* potential together with core-polarization corrections based on a ^{56}Ni core [18]. The low-energy levels known experimentally are not sensitive to all of these parameters, and thus not all of them can be well determined by the selected set of the energy levels. Instead, they are sensitive to certain linear combinations of the parameters. The weights and the number of the most important combinations can be found with the Linear Combination Method (LCD) [19]. Applying LCD for our fit we found that convergence of the χ^2 in the first iteration is achieved already at 20 linear combinations and we have chosen this as a reasonable number for all following iterations. We performed iterations (about six) until the eigen-energies converged. The values of the neutron interaction parameters are adjusted to fit 15 experimental binding energies for $^{57-78}$Ni and 91 energy levels for $^{60-72}$Ni. The nuclei below ^{60}Ni were not emphasized in the fit due to the increased role

TABLE I. Two-body matrix elements $\langle ab;JM|V|cd;JM\rangle$ for protons, neutrons and initial G-matrix. Numbers 1, 2, 3, and 4 corresponds to orbits $f_{5/2}$, $p_{3/2}$, $p_{1/2}$, and $g_{9/2}$, respectively. The single-particle energies for proton orbits are −14.9381, −13.4374, −12.0436, −8.9047. For neutrons they are −9.5134, −9.9883, −8.3608, −5.2546.

a	b	c	d	J	$\langle ab;JM\|V\|cd;JM\rangle$, MeV			a	b	c	d	J	$\langle ab;JM\|V\|cd;JM\rangle$, MeV		
					protons	neutrons	G-matrix						protons	neutrons	G-matrix
1	1	1	1	0	−1.5115	−1.1858	−1.6000	3	2	4	4	2	−0.1630	−0.2714	−0.2560
1	1	2	2	0	−0.6520	−0.7777	−0.8960	4	4	4	4	2	−0.4190	−0.9997	−0.7380
1	1	3	3	0	−0.4862	−0.3517	−0.7210	2	1	2	1	3	0.9435	0.6325	0.2110
1	1	4	4	0	1.7469	1.7963	1.8940	2	1	3	1	3	0.2217	0.1192	0.0860
2	2	2	2	0	−0.7585	−1.1150	−1.0550	3	1	3	1	3	0.9450	0.4571	0.2300
2	2	3	3	0	−0.9686	−1.2807	−1.2900	4	1	4	1	3	−0.0174	-0.1949	−0.2720
2	2	4	4	0	0.7769	1.0202	0.9800	4	1	4	2	3	−0.5309	−0.4843	−0.3960
3	3	3	3	0	0.1755	−0.1057	−0.2500	4	2	4	2	3	−0.6535	−0.7815	−0.8340
3	3	4	4	0	0.8166	0.6105	0.6770	1	1	1	1	4	1.0215	0.3571	0.3820
4	4	4	4	0	−1.1464	−1.3727	−1.2760	1	1	2	1	4	−0.4772	−0.6748	−0.3600
2	1	2	1	1	0.0628	0.0137	−0.1330	1	1	4	4	4	0.1794	0.0652	0.1780
2	1	3	2	1	−0.0183	−0.0119	−0.0250	2	1	2	1	4	0.1113	−0.3549	−0.5280
3	2	3	2	1	0.5854	0.4090	0.1460	2	1	4	4	4	0.4878	0.6141	0.3890
1	1	1	1	2	0.0303	−0.0139	−0.1960	4	1	4	1	4	0.4063	0.3741	0.0650
1	1	2	1	2	−0.1252	−0.2710	−0.0880	4	1	4	2	4	−0.0122	−0.0889	−0.0920
1	1	3	1	2	−0.6649	−0.4778	−0.5010	4	1	4	3	4	−0.0126	−0.0280	−0.1510
1	1	2	2	2	−0.1504	−0.1223	−0.1740	4	2	4	2	4	0.5196	0.1487	−0.0560
1	1	3	2	2	0.3959	0.3409	0.3620	4	2	4	3	4	−0.0074	0.2835	0.2210
1	1	4	4	2	0.3808	0.4163	0.3590	4	3	4	3	4	0.6483	0.2763	−0.0220
2	1	2	1	2	0.4729	0.3812	0.0510	4	4	4	4	4	0.2186	−0.3288	−0.2920
2	1	3	1	2	−0.6090	−0.4652	−0.4320	4	1	4	1	5	0.2025	−0.0589	−0.1730
2	1	2	2	2	−0.1960	−0.1848	−0.1470	4	1	4	2	5	−0.2168	−0.0657	−0.2390
2	1	3	2	2	0.2261	0.2383	0.2210	4	1	4	3	5	−0.2670	−0.3403	−0.4560
2	1	4	4	2	0.3925	0.5906	0.3720	4	2	4	2	5	0.3532	0.0230	−0.1620
3	1	3	1	2	0.0895	−0.1586	−0.4020	4	2	4	3	5	−0.2448	−0.5093	−0.4100
3	1	2	2	2	−0.2590	−0.1790	−0.2050	4	3	4	3	5	0.1861	−0.1653	−0.4600
3	1	3	2	2	0.4675	0.4285	0.4820	4	1	4	1	6	0.6356	0.6235	0.1380
3	1	4	4	2	0.3983	0.5426	0.4820	4	1	4	2	6	−0.2833	−0.5128	−0.0570
4	1	4	1	2	−0.4756	−0.6280	−0.6470	4	2	4	2	6	1.2221	0.4436	0.0190
2	2	2	2	2	0.4458	0.4033	−0.3100	4	4	4	4	6	0.4417	0.1887	−0.0870
2	2	3	2	2	0.6546	0.5159	0.5360	4	1	4	1	7	−0.6009	−0.6491	−1.1290
2	2	4	4	2	0.4390	0.4483	0.3710	4	4	4	4	8	0.6293	0.3245	0.0160
3	2	3	2	2	0.0031	−0.2570	−0.6900	4	4	4	4	8	0.6293	0.3245	0.0160

of excitations from the $f_{7/2}$ orbit as ^{56}Ni is approached [12]. In the absence of experimental data on the binding energy of nuclei near ^{78}Ni we include the SKX [20] Hartree-Fock value of −542.32 MeV for the binding energy of ^{78}Ni as a "data" for the fit. Our calculated binding energies for $^{73-77}$Ni isotopes agree well with the recent corresponding extrapolations from Ref. [21]. For protons 19 binding energies and 113 energy levels were used in a fit (this data set is similar to that used in Ref. [16]). The average deviation in binding and excitation energies between experiment and theory is 241 and 124 keV for neutrons and protons, respectively. Proton, neutron and original G-matrix interactions are summarized in Table I.

III. RESULTS AND DISCUSSION

In this paper we emphasize some of the interesting results for known nuclei and the extrapolation to properties of unknown nuclei. To illustrate some general properties of the new interactions we plot the excitation energies of the 2_1^+ and the 4_1^+ states for neutrons and protons in Figs. 1 and 2, respectively. The systematics shows good agreement between shell-model calculation and experiment. There is some similarity in the trends for the nuclei with $A=68-76$ and $A=90-98$, that is referred to as the VMS [8]. However, the left part of Figs. 1 and 2 ($A=58-66$ for nickel isotopes and $A=80-88$ for $N=50$ isotones) are drastically different. Two

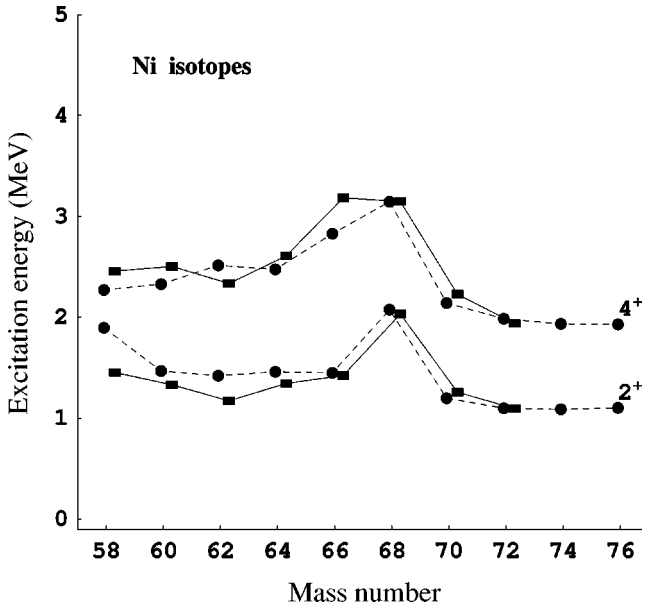

FIG. 1. Calculated and experimental excitation energies of the 2_1^+ and 4_1^+ states in $A=58-76$ even-even nickel isotopes. Calculated levels are given by circles connected by the dashed line. Experimental data are depicted by squares connected by the solid line.

nuclei, ^{66}Ni and ^{88}Sr, show the most profound differences in the location of the 4_1^+ state. The energy gaps between the 4_1^+ and the 2_1^+ states in the ^{62}Ni and the ^{84}Se are also obviously distinct.

These differences may be qualitatively understood from the ordering of the single-particle energies (SPE) for both cases (see Fig. 3). For neutrons the lowest orbital is $p_{3/2}$, which is followed by the $f_{5/2}$, $p_{1/2}$ and $g_{9/2}$ orbitals. This ordering is similar to the familiar cases of interactions in the pf-shell. For the protons we obtain the $f_{5/2}$ orbital as the lowest similar to the previous Ji and Wildenthal interaction

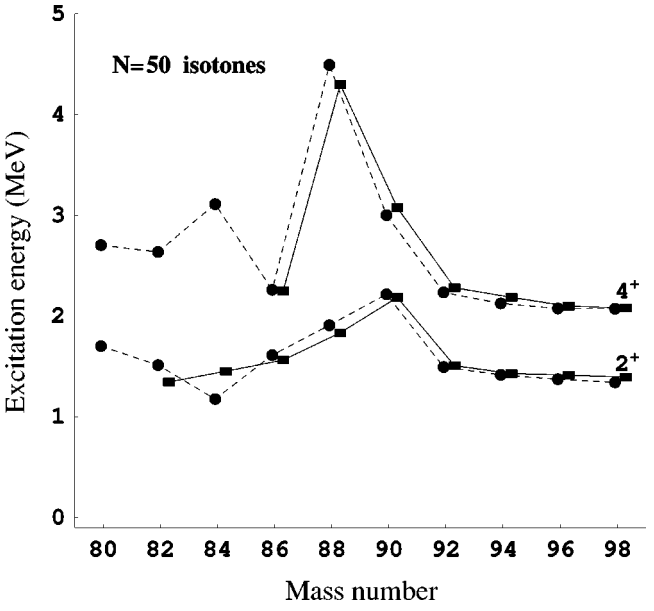

FIG. 2. The same as in the Fig. 1 for $A=80-98$ even-even $N=50$ isotones.

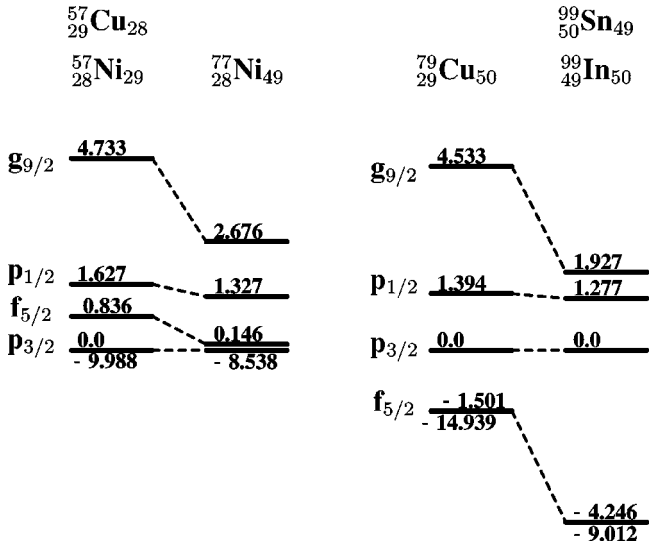

FIG. 3. The neutron (^{57}Ni) and proton (^{79}Cu) single-particle energies (SPE) relative to the ^{56}Ni and the ^{78}Ni cores, respectively. The SPE for neutron holes in ^{78}Ni and proton holes in ^{99}In are also shown. The SPE values relative to the corresponding cores ($p_{3/2}$ orbital) are given below (above) the plotted lines. The relative SPE for ^{57}Cu and ^{99}Sn are similar to those of the mirror nuclei ^{57}Ni and ^{99}In, respectively.

[16]. One notes that the spacing between $p_{3/2}$, $p_{1/2}$ and $g_{9/2}$ is rather similar in both cases. The fact that the $f_{5/2}$ orbital is pushed down in energy in ^{79}Cu relative to ^{57}Cu may be attributed to the neutron mean field of the ^{78}Ni core. The strongly binding monopole interaction in the proton-neutron ($\pi\upsilon$) spin-flip configuration $\pi f_{5/2}\nu g_{9/2}$ as compared to $\pi p_{3/2}\nu g_{9/2}$ causes a dramatic down sloping of the $\pi f_{5/2}$ level in $Z=29$ (Cu) isotopes upon filling of the $\nu g_{9/2}$ orbit [22,23].

The difference in the ordering of the proton orbitals as compared to neutrons is the main reason for the differences (e.g., for the 4^+ states) observed in Figs. 1 and 2. The SPE's impact ground states as well: The $f_{5/2}^6 p_{3/2}^4$ component ($f_{5/2}$ and $p_{3/2}$ are filled) constitutes 59.8% for the ^{88}Sr and only 21.4% for the ^{66}Ni (the VMS partner of the ^{88}Sr). This difference determines what happens beyond the ^{66}Ni (e.g., ^{68}Ni, see also Refs. [6,7]) or ^{88}Sr upon filling the $p_{1/2}$ and the $g_{9/2}$ orbitals.

To compare some overall features of the low energy spectra of the even $^{68-76}$Ni isotopes and even $A=90-98$ $N=50$ isotones we show the calculated and experimental energies for some levels of interest in Figs. 4 and 5, respectively. The energies of the 2_1^+, 4_1^+, 6_1^+ and 8_1^+ states are, approximately, the same in all four $^{70-76}$Ni nuclei. A similar situation holds for the four isotones ^{92}Mo-^{98}Cd, where the validity of the generalized seniority approximation is well established [24]. Indeed, the calculated structure of the wave functions indicate a large contribution of the $g_{9/2}$ orbital for these nuclei. However, this contribution is not so large to conclude the dominance for all four nuclei. This is especially well illustrated by the structure of the ground states: The $[g_{9/2}]_{0^+}^{A-68}$ component in the 0_1^+ wave functions for ^{70,72,74,76}Ni is 44%, 53%, 67% and 83%, respectively. It is obvious that, in contrast to the single $g_{9/2}$ orbital approximation, the structures of

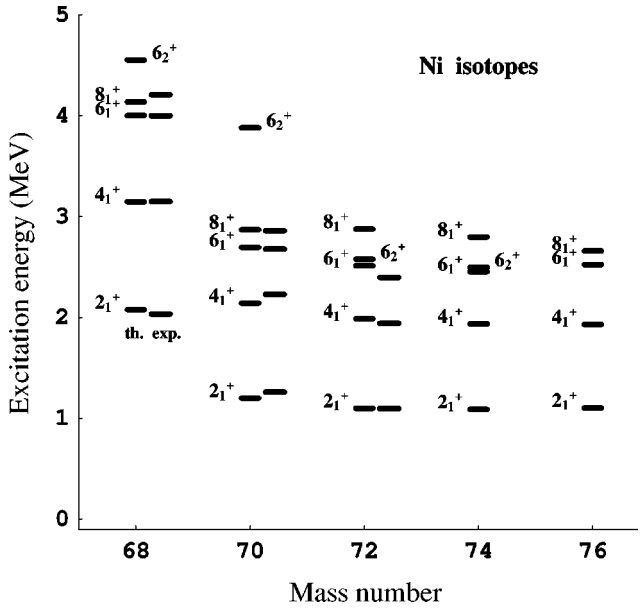

FIG. 4. Yrast level schemes for even-even Ni isotopes with $A=68-76$. Calculated levels on left side and experimental levels on the right side.

^{70}Ni and ^{76}Ni are significantly different. The contributions of the $[g_{9/2}]^{A-68}_{2^+}$ component to the 2^+_1 states have approximately the same weight. The other components of the wave functions play a very important role. For instance, the difference between the effective neutron $g^2_{9/2}$; $J=0$ and $g^2_{9/2}$; $J=2$ TBME's is 0.373 MeV, however, the 2^+-0^+ energy gap in ^{70}Ni or in ^{76}Ni is 1.2–1.1 MeV. Thus the largest contribution to the gap (0.8–0.7 MeV) is mixing with other configurations. The $g_{9/2}$ wave function content of the corresponding valence mirror partners ^{92}Mo-^{98}Cd is slightly larger: 51%, 60%, 71%, and 84% of $[g_{9/2}]^{A-90}_{0^+}$ in the ground states of each

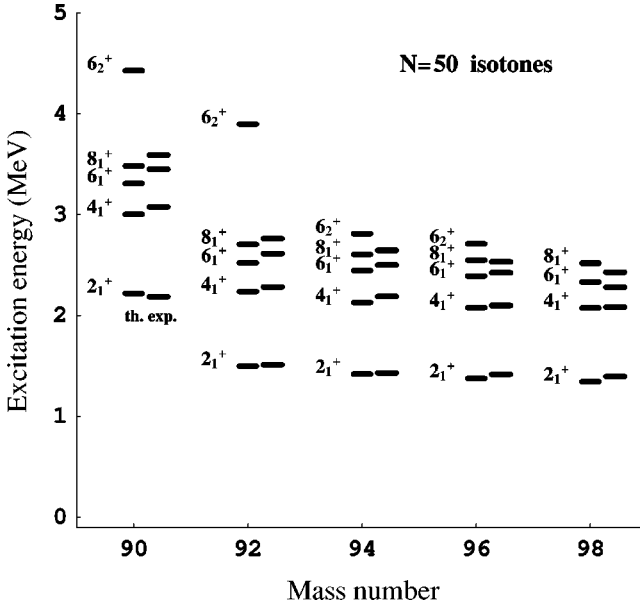

FIG. 5. The same as in the Fig. 4 for even-even $N=50$ isotones with $A=90-98$.

TABLE II. Calculated B(E2; $J^\pi_i \to J^\pi_f$) values for the $A=70-76$ Ni isotopes. A reasonable value of 1.0 is assigned, tentatively, to an effective quadrupole charge e_n. B(E2) values are given in units of e^2+fm^4. Calculated and available experimental lifetimes τ for the 8^+_1 state are given in last two rows. Experimental excitation energies were used in lifetime calculations for ^{70}Ni. For ^{72,74,76}Ni isotopes theoretical excitation energies were used.

J^π_i	J^π_f	^{70}Ni	^{72}Ni	^{74}Ni	^{76}Ni
2^+_1	0^+_1	64	84	76	46
4^+_1	2^+_1	51	94	85	54
6^+_1	4^+_1	31	29	34	37
8^+_1	6^+_1	12	1.9	9.2	15
	6^+_2	3.3	52	47	⋯
$\tau(8^+_1)$	Th.	326.0 ns	6.1 ns	5.1 ns	1.2 μs
	Expt.	335(4)[a] ns	<26[b] ns	<87[b] ns	

[a]Reference [2].
[b]Reference [4].

A-isotone, respectively, but the overall situation is rather similar to ^{70,72,74,76}Ni. The energies of the 2^+_1 states for the nickel isotopes are systematically lower ($\sim$0.3 MeV) than for the $N=50$ isotones. This effect is due to the properties of effective $g^2_{9/2}$ TBME's, since the energy gap between the effective $g^2_{9/2}$; $J=0$ and $g^2_{9/2}$; $J=2$ TBME's is 0.727 and 0.3 MeV for protons and neutrons, respectively (i.e., they differ by approximately the same $\sim$0.373 MeV) and the calculated structure of the $^{70-76}$Ni and ^{92}Mo-^{98}Cd is similar (the energy gap in the starting renormalized Bonn-C Hamiltonian is 0.538 MeV). We interpret this as an indication that the $Z=28$ proton shell gap near ^{68}Ni is relatively weak compared to the $N=50$ neutron shell gap near ^{88}Sr. Thus, the nuclei $^{56-78}$Ni have substantial amounts of proton core excitations that are not included explicitly in the model space, but are implicitly taken into account by the effective TBME. In a potential model one would expect that the proton-proton TBME for $N=50$ are related to the neutron-neutron TBME for $Z=28$ with the subtraction of the Coulomb interaction and perhaps some overall mass scaling. But we have found that this approach does not work, presumably due to the difference in the core-polarization contributions between the regions of ^{68}Ni and ^{88}Sr (the original G matrix from Hjorth-Jensen [18] contains an approximate core-polarization correction for an assumed ^{56}Ni core).

The lowering of the effective $J=2$-$J=0$ gap for the nickel isotopes compared to $N=50$ has important consequences for non-yrast states. This is illustrated by the properties of the 6^+ states. For ^{94}Ru and ^{96}Pd the second 6^+ state is dominantly seniority $\nu=4$ and lies above the 8^+_1 state, while in ^{72}Ni and ^{74}Ni it is well below the 8^+_1 state and is almost degenerate with the 6^+_1 seniority $\nu=2$ state. Despite the very small splitting between two 6^+ states with dominant seniority $\nu=2$ and $\nu=4$ they are only slightly mixed. The structure and location of the 6^+ states has important implications for the isomeric properties of the 8^+ states. The B(E2; $8^+_1 \to 6^+_{1,2}$) values are given in Table II. The E2 transition between the 8^+ and 6^+ states of the same seniority is forbidden in the middle of the shell. It is well known that this seniority selection rule leads

TABLE III. Calculated and experimental B(E2; $J_i^\pi \to J_i^\pi - 2$) values for $A=92-98$, $N=50$ isotones. A reasonable value of 2.0 is assigned, tentatively, to an effective quadrupole charge e_p [24]. B(E2) values are given in e^2fm^4 units.

J_i^π	^{92}Mo		^{94}Ru		^{96}Pd		^{96}Cd	
	Th.	Expt.[a]	Th.	Expt.[a]	Th.	Expt.[a]	Th.	Expt.[b]
2_1^+	235	207(12)	304	⋯	283	⋯	181	⋯
4_1^+	164	<605	9.2	⋯	40	⋯	214	⋯
6_1^+	110	81(2)	8.2	2.9(1)	20	20(3)	149	⋯
8_1^+	42	32.4(5)	2.7	0.09(1)	7.1	8.9(12)	60	35(11)

[a]Reference [25].
[b]Reference [26].

to the isomerism of 8_1^+ states in ^{94}Ru and ^{96}Pd [25], with measured lifetimes τ of 102(6) and 3.2(4) μs, respectively. Our calculations result in lifetimes of the order of μs as well (see Table III). The discrepancy between theoretical and experimental B(E2) values for the ^{94}Ru is relatively large, and this is common to previous calculations [17,24].

Turning back to Ni-isotopes, one notes, that pushing down of the 6_2^+ $v=4$ states opens up a new channel for the fast E2 decay of the 8^+ states that results in the disappearance of isomeric states in ^{72,74}Ni–the corresponding lifetimes move down to the ns region (see Table II). Our results with the newly derived interactions fully support the above explanation of the absence of an isomeric 8^+ state in ^{72}Ni proposed in Refs. [3,4] on the basis of single $g_{9/2}$ orbital shell-model calculations since our calculated wave functions of the $8^+, 6^+$ states in ^{72,76}Ni are dominated by the $g_{9/2}^4$ (70%) and $g_{9/2}^6$ (85%) configurations, respectively. However, it is shown above that this is not the case for the 0_1^+ and 2_1^+ states.

IV. CONCLUSION

Clearly more detailed experimental studies of the nuclei in the vicinity of the ^{78}Ni are required to verify the shell-model predictions. The next step will be to combine these new neutron-neutron and proton-proton effective Hamiltonians with a proton-neutron Hamiltonian to describe the wide variety of spherical, collective and co-existing features for the $A=56-100$ mass region as well as to apply the wave-functions to the calculations of weak-interaction and astrophysical phenomena.

ACKNOWLEDGMENT

We acknowledge support from NSF Grant No. PHY-0244453.

[1] R. Broda *et al.*, Phys. Rev. Lett. **74**, 868 (1995).
[2] R. Grzywacz *et al.*, Phys. Rev. Lett. **81**, 766 (1998).
[3] H. Grawe, Nucl. Phys. **A704**, 211c (2002).
[4] M. Sawicka *et al.*, Phys. Rev. C **68**, 044304 (2003).
[5] T. Ishii *et al.*, Phys. Rev. Lett. **84**, 39 (2000).
[6] O. Sorlin *et al.*, Phys. Rev. Lett. **88**, 092501 (2002).
[7] K. Langanke *et al.*, Phys. Rev. C **67**, 044314 (2003).
[8] R. Wirowski *et al.*, J. Phys. G **14**, L195 (1988).
[9] B. A. Brown and B. H. Wildenthal, Annu. Rev. Nucl. Part. Sci. **38**, 29 (1988).
[10] A. Poves *et al.*, Nucl. Phys. **A694**, 157 (2001).
[11] M. Honma *et al.*, Phys. Rev. C **65**, 061301(R) (2002).
[12] M. Honma *et al.*, Phys. Rev. C **69**, 034335 (2004).
[13] T. Otsuka *et al.*, Prog. Part. Nucl. Phys. **47**, 319 (2001).
[14] M. Horoi, B. A. Brown, and V. Zelevinsky, Phys. Rev. C **67**, 034303 (2003).
[15] H. Grawe, Prog. Part. Nucl. Phys. **38**, 15 (1997).
[16] Xiangdong Ji and B. H. Wildenthal, Phys. Rev. C **37**, 1256 (1988).
[17] J. Sinatkas *et al.*, J. Phys. G **18**, 1377 (1992).
[18] M. Hjorth-Jensen, private communication.
[19] M. Honma *et al.*, Nucl. Phys. **A704**, 134c (2002).
[20] B. A. Brown, Phys. Rev. C **58**, 220 (1998).
[21] G. Audi, A. H. Wapstra, and C. Thibault, Nucl. Phys. **A729**, 337 (2003).
[22] H. Grawe *et al.*, Acta Phys. Pol. B **34**, 2267 (2003).
[23] S. Franchoo *et al.*, Phys. Rev. C **64**, 054308 (2001).
[24] Xiangdong Ji and B. H. Wildenthal, Phys. Rev. C **38**, 2849 (1988).
[25] ENSDF, http://www.nndc.bnl.gov/nndc/ensdf/
[26] A. Blazhev *et al.*, Phys. Rev. C **69**, 064304 (2004).